Formation of secondary organic aerosols from the ozonolysis of dihydrofurans.

Diaz-de-Mera, Yolanda[1]; Aranda, Alfonso[1]; Bracco, Larisa[2]; Rodriguez, Diana[3]; Rodriguez, Ana[3].

[1]Universidad de Castilla-La Mancha. Facultad de Ciencias y Tecnologias Quimicas. Avenida Camilo José Cela s/n, 13071. Ciudad real. Spain.

[2]Instituto de Investigaciones Fisicoquímicas Teóricas y Aplicadas (INIFTA), Departamento de Química, Facultad de Ciencias Exactas, Universidad Nacional de La Plata, CONICET, Casilla de Correo 16, Sucursal 4, La Plata 1900, Argentina.

[3]Universidad de Castilla-La Mancha. Facultad de Ciencias Ambientales y Bioquimica. Avenida Carlos III s/n, 45071 Toledo, Spain.

Correspondence to: Alfonso Aranda (alfonso.aranda@uclm.es)

Abstract. In this work we report the study of the ozonolysis of 2,5-dihydrofuran and 2,3-dihydrofuran and the reaction conditions leading to the formation of secondary organic aerosols. The reactions have been carried out in a Teflon chamber filled with synthetic air mixtures at atmospheric pressure and room temperature. The ozonolysis only produced particles in the presence of SO_2. Rising relative humidity from 0 to 40% had no effect on the production of secondary organic aerosol in the case of 2,5-dihydrofuran while it reduced the particle number and particle mass concentrations from the 2,3-dihydrofuran ozonolysis. The water and SO_2 rate constants ratio for the 2,3-dihydrofuran Criegee intermediate was derived from the SOA yields in experiments with different relative humidity values, $k_{H2O}/k_{SO2}= (9.8\pm3.7)\times10^{-5}$.

The experimental results show that SO_3 may not be the only intermediate involved in the formation or growth of new particles in contrast to the data reported for other Criegee intermediates/SO_2 reactions. For the studied reactions, SO_2 concentrations remained constant during the experiments behaving as a catalyst in the production of condensable products. Computational calculations also show that the stabilised Criegee intermediates from the ozonolysis reaction of both 2,5-dihydrofuran and 2,3-dihydrofuran may react with SO_2 resulting in the regeneration of SO_2 and the formation of low-volatility organic acids.

Introduction.

Recent years have seen a growing interest in the atmospheric mechanisms leading to the formation of secondary organic aerosols, SOA (Chan et al., 2010). In this sense, ozonolysis of terpenes has been reported as a potential source of new particles under natural conditions (Saathoff et al., 2009; Sipilä et al., 2014; Newland et al., 2015a). The oxidation of terpenes leads to the formation of extremely low-volatility organic compounds that can enhance or even dominate the formation and growth of organic aerosol particles in forested areas. Dimers of these species are considered large enough to act as nano-condensation

nuclei (Ehn et al., 2014). Likewise, the fast reactions of other alkenes with ozone can contribute to the production of non-volatile species that could condense and contribute to the total mass of pre-existing particles or even induce nucleation events in both rural and urban atmospheres.

As it is known (Johnson and Marston, 2008), ozone adds to the double bond giving an energy-rich primary ozonide which promptly decomposes giving a carbonyl molecule and an excited carbonyl oxide reactive intermediate (Criegee Intermediate, CI). For cyclic alkenes, the ozonolysis just opens the cycle giving larger CI compared to the equivalent linear alkenes. Furthermore, the carbonyl functional group is included in the CI molecule. Thus, products with higher molecular weight, lower volatility and higher potential capacity to contribute to SOA formation are expected for chemicals with endocyclic double bonds. The excited CI intermediate can be stabilised by collisions with gas molecules or undergo fragmentation or unimolecular rearrangement (Anglada et al., 2011). Then, the stabilised CI (sCI) can react with other molecules in the gas phase such as H_2O, HO_x, aldehydes, organic acids, RO_2, NO_x, etc (Vereecken et al., 2012). The reaction with water molecules is expected to be one of the main fates of sCI, giving α-hydroxi-hydroperoxides (Ryzhkov and Ariya 2004; Anglada et al., 2011).

On the other hand, experimental results show that SO_2-sCI reactions are a potential source of SOA. Very recently, it has been found that a significant fraction of ground level sulfuric acid originates from the oxidation of sulphur dioxide by sCI to SO_3 (Mauldin et al., 2012) and, thus, several studies have been carried out on the reactions of Criegee intermediates with SO_2 (Boy et al., 2013; Berndt et al., 2014a; Stone et al., 2014; Newland et al., 2015b; Liu et al., 2016). The relative contribution of SO_2 and water vapour to the CI removal in the atmosphere depends on the CI structure (Berndt et al., 2014a; Stone et al., 2014) and may have an important effect on the SOA formation yields.

In this work we report the study of the ozonolysis of 2,5-dihydrofuran (2,5-DHF) and 2,3-dihydrofuran (2,3-DHF) under variable concentrations of water vapour and SO_2.

2,5-DHF + O_3 →… SOA   (R1)

2,3-DHF + O_3 →… SOA   (R2)
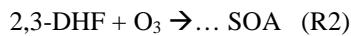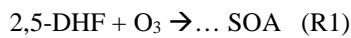
Very recently, it has been found that different dihydrofurans may be involved in the SOA formation from alkane photooxidation (Loza et al.,2014; Zhang et al., 2014). Alkoxy radicals are initially generated from the reaction with OH. They can subsequently isomerize into δ-hydrocarbonyl intermediates which undergo cyclization and dehydration producing dihydrofurans (Martín et al., 2002).

2,3-dihydrofuran is also found in the atmosphere due to the emissions from biomass burning (Lemieux et al., 2004) and is included in atmospheric chemistry models aimed at the emissions of aerosols (Freitas et al., 2011). Furthermore, during the last few years, different oxygenate chemicals are being tested as fuel additives or components of biofuels. Thus, furans and derivatives are potential second-generation biofuels since they could be produced from fructose and glucose. (Román-Leshkov

et al., 2007). In this sense, the ignition characteristics of 2,5-DHF have been reported and compared to those of other heterocyclic compounds (Fan et al., 2016).

A previous work has reported the tropospheric oxidation study of 2,5-DHF and 2,3-DHF (Alwe et al., 2014). The measured rate constants with ozone are: 1.65 and 443.2 $\times$ 10^{-17} cm^3 molecule^{-1} s^{-1} for 2,5-DHF and 2,3-DHF, respectively. Alwe et al. (Alwe t al., 2014) show that the dominant pathway of tropospheric degradation of 2,5-DHF is the reaction with OH, whereas for 2,3-DHF is the reaction with O_3. So, ozonolysis of 2,3-DHF is a potential source of CI in the troposphere. Although the reaction of 2,5 DHF with ozone is slower, the result for this unsaturated cyclic ether may serve as reference for other substituted dihydrofurans.

Up to now, no previous studies have been carried out to assess the potential capacity of the title compounds to generate condensable matter and SOA. Thus, in this work we study the ozonolysis reactions of 2,5-DHF and 2,3-DHF following the conditions that lead to the formation and growth of new particles. The effect of water vapour and SO_2 concentrations during the process are also studied and discussed. The experimental work is supported by theoretical calculations to explore the key steps involved within the reaction mechanism leading to SOA.

2. Methods and instrumentation:

2.1. Experimental set-up and methods.

A schematic diagram of the experimental system is shown in Fig. 1. A 200L capacity FEP collapsible chamber has been used to carry out most of the experiments under atmospheric pressure at 297±1K. The reactants were sequentially sampled in a volume-calibrated glass bulb (1,059L) using capacitance pressure gauges, MKS 626AX, 100 and 1000Torr full scale, and then flushed to the reactor using synthetic air through a mass flow controller, MFC 1179BX, MKS. The concentrations of each substance were calculated from their partial pressure in the bulb and the dilution factor considering the glass bulb volume and the final volume of the Teflon reactor.

Ozone was produced by an ozone generator, BMT Messtechnik 802N, fed with pure oxygen. The ozone/oxygen mixture was introduced simultaneously to the sampling bag and to a 19.8 cm long quartz cell to measure the absorption of radiation at 255nm using a UV-vis Hamamatsu spectrometer, C10082CAH, with a 1 nm resolution. The ozone concentration in the bulb was then calculated from the known value of the ozone absorption cross section. Further dilution of ozone enabled the required range of ozone concentrations in the reactor.

Water vapour was generated using a glass bubbler placed just before the reactor inlet. The amount of water required for a given relative humidity was calculated and injected in the bubbler. All the sampled water was then evaporated and flushed inside the reactor through the flow of synthetic air.

The certified water impurity content in the synthetic air used was below 2ppm. Although it is generally negligible, it could be significant if water molecules were involved in fast reactions. To properly asses the effect of water in the studied reactions, for

the experiments at HR=0%, the flow from the air cylinder was passed through a trap containing molecular sieve 5A (Supelco) cooled down to 157K with an ethanol-liquid nitrogen slush bath. Some experiments were also carried using a liquid nitrogen trap and checking that no condensed oxygen was visible in the trap. For such experiments water concentration in the reactor was estimated as low as 20 ± 10ppb by introducing the dried air and known concentrations of SO_3 and monitoring the time for

5   new particle formation (see supplementary material, Fig. S1 and related discussion).

The sequence of reactants entering the Teflon bag was as follows. First, 2,5-DHF (or 2,3-DHF) was introduced, then the OH scavenger (cyclohexane), then SO_2 and finally ozone. In the experiments carried out with water vapour, water was introduced in the bubbler at the beginning, being evaporated by the air carrying the DHF, the scavenger and SO_2.

The injection of ozone constitutes the ignition of the 2,5-DHF (or 2,3-DHF)–ozone reaction. To completely wash away the

10   ozone from the bulb and transport it to the reactor, a flow of synthetic air was required for 45 seconds. During this time period the Teflon reactor was shaken to accelerate the mixing of reactants.

The formation of particles was followed continuously by a CPC particle counting 3775 TSI and, at given times, samples were derived to a fast mobility particle sizer (FMPS 3091,TSI) to obtain the particle size distribution and total mass of particles with diameters within the range 5.6–560 nm (Aranda et al., 2015). The total aerosol mass concentration was calculated from the

15   measured particle size distribution assuming unit density and spherical particles.

Prior to each experiment the Teflon bag was repetitively filled and emptied with clean synthetic air to remove particles remaining from previous experiments. The process was continued until the level of particles was below 1 #cm^{-3}.

For some experiments, a fluorescence SO_2 analyser, Teledyne Instruments 101-E, was coupled to the reactor to measure the SO_2 concentration profiles during the experiments. Previous runs with only SO_2 /air samples in the reactor showed that SO_2

20   wall losses were negligible. Additionally, no interference in the SO_2 fluorescence signal from the rest of co-reactants was observed in the range of concentrations used in this study.

A series of experiments was also carried out monitoring the O_3 concentration using an ozone analyser, Environment O342M to follow the decay of O_3 and validate the simulated decays of reactants due to the ozonolysis reactions.

2.2. Computational methods.

25   All the calculations were performed with the Gaussian09 program package (Frisch et al., 2009). The BMK formulations (Boese and Martin, 2004) of the density functional theory (DFT) combined with the Pople triple split-valence basis set 6-311++G(3df,3pd) were employed. In all cases, the structural parameters were fully optimized via analytic gradient methods. The Synchronous Transit-Guided Quasi-Newton (STQN) method was employed for locating transition structures. For a better estimation of energies, single point calculations at ab initio level CCSD(T) were performed using the 6-311G(d,p)

30   basis set (Cizek, 1969; Bartlett, 1989).

2.3 Reagents.

All the substances used were of the highest commercially available purity. Liquid reagents were purified by successive trap to trap distillation. 2,5-DHF 97%, Aldrich; 2,3-DHF 99%, Aldrich; SO_2 99,9%, Fluka; cyclohexane 99.5%, Sigma-Aldrich; synthetic air 3X, Praxair; O_2 4X, Praxair. SO_3, Sigma-Aldric>99%.

3. Results and discussion.

3.1. 2-5-Dihydrofuran.

3.1.1. Conditions for SOA formation.

Cyclohexane in excess was used as OH radical scavenger in concentration ratios so that >95% of OH formed in the reactions was removed (Ma et al., 2009). Different series of experiments were carried out to characterize the formation and growth of particles originated from the reaction of ozone with 2,5-DHF.

In Fig. 2 we show a typical experiment carried out with 0.5ppm of 2,5-DHF, 1ppm of O_3 and 0.5ppm of SO_2 with zero relative humidity (RH) initial concentrations. Since new particles are readily formed due to this reaction, low volatile substances must be produced and over-exceed several times their saturation vapour pressure, initiating homogeneous nucleation (Kelving effect) (Pruppacher et al., 1998). The experimental data obtained for the particle number concentration are presented together with the simulated profile of 2,5-DHF (from the known initial concentrations and the gas-phase rate constant (Alwe et al., 2014), the experimental and simulated ozone profiles and the total concentration of consumed 2,5-DHF, Fig. 2. Small particles with diameters above 4nm were quickly detected by the CPC. A maximum in the particle number concentration (PNC) was observed around 8 minutes and then PNC progressively decreased with time mainly due to coagulation of particles and wall losses. For reaction times longer than 2 hours and PNC below $1x10^4$#cm^{-3} its decrease may be attributed solely to wall losses. The plot of Ln(PNC) against time for different experiments provided linear fittings and an average K_w of $(5\pm2)\times10^{-5}s^{-1}$.

The total mass concentration (or particle mass concentration, PMC) of measured aerosol is also shown in Fig. 2 multiplied by a factor scale since the units are different to the rest of magnitudes. The PMC profile arises after the nucleation event and continues growing until approximately 30 minutes. Then a low decrease of the mass concentration is observed with time. The profile of total concentration of consumed 2,5-DHF is very similar to that of the mass concentration. This fact suggests that reaction (R1) is the limiting step in the production of condensable matter. Beyond 30 minutes the mass concentration decreases, mainly due to wall losses, although 2,5-DHF is still reacting. Better fits of these two profiles are obtained when the wall rate constant is considered.

A series of experiments with lower concentrations of reactants was conducted to characterize the nucleation conditions. Thus, for example, in Fig. 2 we can also see the profile of the particle number concentration for initial concentrations of 2,5-DHF, ozone and SO_2 0.1, 0.2 and 0.1 ppm, respectively. In such experiment no particles were detected before 3 minutes total time.

For such reaction time and conditions, the reacted concentration of 2,5-DHF amounts 3.5×10^{10}molecule cm^{-3}. From the average of the different experiments, we estimate that an upper limit concentration of $3.5 \pm 1 \times 10^{10}$molecule cm^{-3} is required for the direct gas-phase product from reaction (R1) to originate the nucleation event.

3.1.2. Effect of SO$_2$ and water.

5   When the experiments were carried out in the absence of SO$_2$, no particles were observed. On the other hand, when SO$_2$ was added, an increase in PNC and in the total condensed mass is observed for increasing concentrations of SO$_2$, Fig. S2 (supplementary material). Even for relatively low SO$_2$ concentrations high concentrations of particles (above 10^5 #cm^{-3}) were measured. This series of experiments was conducted with dried synthetic air with water concentration around 20ppb.

A series of experiment was conducted also following the temporal profile of SO$_2$ for initial concentrations in the range 0.5

10   ppm down to 10ppb and higher 2,5-DHF and ozone concentrations, in the range of 0.5 to 1 ppm. In all cases the SO$_2$ concentration remained neatly constant during these experiments (Fig. S3, supplementary material) showing that, although sulphur dioxide participates in the mechanism leading to particles, it is released again as free gas-phase SO$_2$.

From the experimental SO$_2$ profiles a first order loss rate constant may be inferred. For example from the experiments with 10ppb of SO$_2$, k= 8.5×10^{-6}s^{-1}. To check the possibility of SO$_3$ production, we can assume a simple mechanism where any lost

15   SO$_2$ molecule would be converted exclusively into SO$_3$:

SO$_2$ → SO$_3$ k= 8.5×10^{-6}s^{-1}
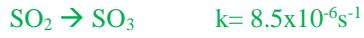
And then SO$_3$ would exclusively react with water to produce H$_2$SO$_4$:

H$_2$O + SO$_3$ → H$_2$SO$_4$ k= 3.90×10^{-41}exp(6830.6/T)[H2O]^2 (Jayne et al., 1997).

Simulating the SO$_2$, SO$_3$ and H$_2$O profiles for a 20ppb water concentration and for 10 ppb initial SO$_2$ concentration, it would

20   require more than 1 hour to generate 5×10^6molecule cm^{-3} of H$_2$SO$_4$, which is the approximate concentration able to nucleate (Metzger et al., 2010). For 20ppb initial SO$_2$ concentration it would require 28 minutes. Nevertheless, for these experiment nucleation was almost instantaneous if we take away the mixing time of reactants. So, for the experiments with the lower concentrations of SO$_2$, the results suggest that the reaction of SO$_3$ with water cannot be responsible for the formation of particles and that an alternative "dry channel" is able to produce organic non-volatile species able to condense. For higher

25   SO$_2$ concentrations (in the range of 0.5 ppm) small changes at the level of the uncertainty of the SO$_2$ measurements can not be completely excluded as a possible source of SO$_3$.

Under atmospheric conditions, reactions with water vapour is expected to be one of the main fates of CI intermediates (Ryzhkov and Ariya, 2004). For 2,5-DHF, Fig. S4 shows that increasing the RH within the range 0 to 40% had no significant effect in the measured values of both PNC and PMC. Thus, concerning the potential competing reactions of the sCI with water

30   vapour and SO$_2$, the results suggest that water reaction contribution is negligible.

Concerning the effect of ozone and 2,5-DHF initial concentrations, different series of experiments were carried out. As discussed above, the ozone reaction with 2,5-DHF was the rate limiting step in the production of SOA. Thus, the increase of $[O_3]$ or [2,5-DHF] led to the acceleration of the process and the increase of the measured PNC and PMC. See supplementary information, Fig. S5-S7, for further details.

5   ## 3.2. 2,3-Dihydrofuran.

3.2.1. Effect of SO_2.

In Fig. 3 and S8 we show the results for a typical experiments carried out with 1 ppm of ozone and 0.5 ppm of 2,3-DHF with dried synthetic air. When the experiments were carried out in the absence of SO_2, no particles were observed. On the other hand, when SO_2 was added as co-reactant (see for example the profile of the experiment with 0.5 ppm initial concentrations

10   of SO_2 and 0% HR) particles suddenly originated after approximately 1 minute after the introduction of ozone in the reactor. The number of particles still grew until approximately 5 minutes and then decreased during the rest of the experiment. In Fig. 3 we can also see the experimental O_3 profile and the simulated profile for [2,3-DHF]. The ozone-2,3-DHF reaction is very fast and 2,3-DHF is consumed within the first minute of the experiment while the mass of condensed matter starts growing after nucleation and continues beyond 20 minutes. These results show that the initial ozone-2,3-DHF reaction itself is not the

15   rate limiting step in the mechanism leading to new particles, in contrast to the results for 2,5-DHF. For experiments with increasing concentrations of SO_2, nucleation was found at shorter times and higher PNC values were obtained. The total mass and diameter of particles also increased with SO_2, Fig. 3 and Fig. S9. For the smaller SO_2 concentration, (0.05ppm) a clear delay of the burst of nucleation is observed, Fig. 3. These results suggest that SO_2 is involved within the first steps of the mechanism driving to the nucleation event. For such reason the potential secondary ozonide formed

20   from the sCI reaction with SO_2 has been characterized, see below. A series of experiment was conducted following the temporal profile of SO_2 for initial concentrations in the range 0.01 to 0.5ppm and higher 2,3-DHF and ozone concentrations (0.5 to 1 ppm, respectively). As in the case of reaction (R1), for reaction (R2) the SO_2 concentration remained constant during these experiments. Likewise, SO_3-water reaction is not expected to contribute to nucleation, at least in the experiments with SO_2 below 0.02ppm. The facts that new particles are generated only

25   in the presence of SO_2 and that SO_2 does not decrease during the experiments suggest that sulphur dioxide can behave as a catalyst in the production of condensable products leading to particles.

3.2.2. Effect of 2,3-DHF and ozone initial concentrations.

Two series of experiments were carried out changing the ratio of 2,3-DHF over ozone for a fixed concentration of SO_2 and in the absence of water vapour. The results are summarized in Table 1. When 2,3-DHF was in excess over ozone, it led to a fast

consumption of ozone (during the first minute). As show in the table, for a fixed low initial ozone concentration, the higher the concentration of 2,3-DHF, the lower the number concentration. Nucleation in these experiments (hardly observed) was also almost instantaneous but the PNC significantly decreased (at least two orders of magnitude) compared to the reference experiments (stoichiometric conditions) and the total mass fell to virtually zero. For those experiments, a significant difference

5   was observed in the number concentration data from the FMPS and the CPC. The FMPS hardly detected particles (they must have diameters above 5.6nm to be detectable) while the CPC can detect smaller particles (down to 4 nm). The results showed that the particles did not grow when ozone was the stoichiometry limiting reactant. Thus, further ozone may be involved after the initial O_3-2,3-DHF reaction to produce SOA. These results are also consistent with the series of experiments with ozone in excess over 2,3-DHF. With ozone in excess, the particle number concentration and the total mass of particles increased with

10   the ozone concentration. As found in Table 1 or Fig. S10, the size of the particles also grew as the initial ozone concentration was increased.

3.2.3. Effect of water vapour.

Two series of experiments have been carried out in this work to study the effect of water. First, for the experiments conducted in the presence of water (RH from 0 to 50%) and in the absence of SO_2, no particle formation was observed. So, if water reacts

15   with the 2,3-DHF CI, this reaction does not produce particles in the absence of SO_2, Table S1 (supplementary material). In the second series of experiments SO_2 was also present, being all the experiments carried under the same initial concentrations of 2,3-DHF, ozone and SO_2 with HR ranging from 0 to 50%. As shown in Fig. 4 and Fig. S11, the increase in RH reduced the particle number concentration and the mass of formed SOA. Figure 4 shows the results for two experiments, under dried air conditions and under 50% RH. In the presence of 50% HR, the particle number concentration was significantly lower and the

20   measured mass concentration fell from 13 to approximately 3 µg cm^{-3}. Concerning the growth of particles, their final diameters were also smaller in the presence of water.

These effects may be due to the reaction of water with the Criegee intermediate which would compete with the sCI reaction towards SO_2. From previous studies, (Anglada et al., 2011) this reaction is expected to proceed through the addition of the water oxygen atom to the carbon atom in the carbonyl oxide and the simultaneous transfer of one hydrogen atom from the

25   water molecule to the terminal O atom in the CI. The expected products are α-hydroxi-hydroperoxides that can subsequently decompose or react with other atmospheric species.

If we take the dry experiments (0% HR) as reference, then we can assume that for the experiments carried out in the presence of water the decrease in mass concentration, Δ_{PMC}, is due exclusively to the reaction of water molecules with the sCI. Water would competitively consume sCI, with a kinetic rate constant k_{H2O}, against the reaction with SO_2, with a kinetic rate constant

30   k_{SO2}. Thus, the ratio $(k_{H2O}.[H_2O])/(k_{SO2}.[SO_2])$ can be obtained from the ratio Δ_{PMC} /PMC, that is, from the drop in the mass concentration values measured at a given relative humidity (Δ_{PMC} drop is attributed solely to the reaction with H_2O) and the

actual mass concentration obtained in such conditions (PMC, attributed to the reaction with SO_2). Thus, the ratio for the rate constants of the 2,3-DHF Criegee intermediate with water vapour and SO_2 was obtained plotting Δ_{PMC} /PMC versus $[H_2O]$ for constant and known SO_2 concentration (Fig. S12), k_{H2O}/k_{SO2}= $(9.8\pm3.7)\times10^{-5}$. This ratio is similar to other reported values for different CI, (Berndt et al., 2014a). This result may be used to assess different atmospheric conditions. For example, for

5   relatively dry conditions (20% HR) in a polluted atmosphere with 75 ppbs of SO_2 (the current 1 hour NAAQS standard) at 25ºC, approximately 11% of the sCI produced in the ozonolysis of 2,3-DHF would react with SO_2 with potential to yield new particles and nucleation events. In the lower troposphere this source is not unique in the sense that other pollutants would be simultaneously producing condensable products. Nucleation under real atmospheric conditions is due to the cumulative sources of non-volatile species and so these events are expected to generate under lower concentrations than those found in the

10   laboratory for the individual sources.

3.3. Theoretical insights.

Recent studies have revealed that sCI may react with SO_2 and other trace gases several orders of magnitude faster than assumed so far (Welz et al., 2012). Therefore sCI reactions have emerged as a potential source of tropospheric sulphate to be assessed in the predictions of tropospheric aerosol formation. Even though the atmospheric fate of the smaller carbonyl oxides is mainly

15   dominated by the reaction with water molecules or water dimers, (Berndt et al., 2014a; Chao et al., 2015), the reactivity of sCIs is strongly dependent on the structure.

Previous theoretical studies have shown that the first step of the sCI with SO_2 is the formation of a cyclic secondary ozonide (SOZ) that can undergo decomposition to the corresponding carbonyl and SO_3 or isomerization involving a 1,2-H-shift leading to an organic acid and SO_2 (Jiang et al., 2010; Kurten et al., 2011). The release of SO_3 would produce H_2SO_4 in the presence

20   of water molecules. Vereeken et al. (Vereeken et al., 2012), also described the formation of a stable ester sulfinic acid from the opening of the SOZ.

$R_1R_2COO + SO_2 \rightarrow R_1R_2CO + SO_3$ (R3)

$\rightarrow R_1COOH + SO_2$ (only if R_2 = H)   (R4)

$\rightarrow R_1C(O)OS(O)OH$ (only if R_2 = H)   (R5)
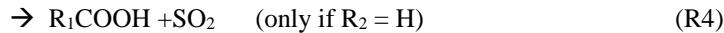
25   In this sense we have studied the transition states for both 2,5-DHF and 2,3-DHF Criegee intermediates reactions with SO_2. Figure 5a shows a schematic representation of the general potential energy surface for the studied reactions. Figure 5b displays the optimized geometries of the stationary points for all reactants, products and stationary states from the sCI obtained at BMK/6-311++G(3df,3pd) level of theory. The sCI +SO_2 system has been taken as zero energy reference. As, shown in Table 2, the first step of the ozonolysis is highly exothermic, so unimolecular decomposition and stabilisation through collision

30   would compete in the formation of both sCI. Concerning the reaction mechanism, In the case of 2,5-DHF reaction with O_3,

only one Criegee intermediate (sCI1) may be formed. On the other hand, due to the asymmetry of 2,3-DHF, two possible Criegee intermediates can be obtained (sCI2 and sCI3) from its reaction with O_3. For all these intermediates, there are two possible configurations, syn and anti. The latter, anti, were used in all cases to perform the potential energy surface calculations since they were more stable than the syn isomers in 1.08, 3.67 and 3.65 kcal mol^{-1}, respectively.

5   The reaction of sCI1 with SO_2 first evolves to the formation of an intermediate adduct M1, which then may react through two channels. On the one hand, through the transition state TS1.1, SO_3 and an aldehyde are formed. If the adduct M1 evolves via the transition state TS1.2, SO_2 is regenerated and an organic acid is produced. Due to the fact that both transition states lie below the energy of reactants, the most favourable reaction results in the regeneration of SO_2 and the organic acid with reaction energy of -117.58 kcal mol^{-1} , Table 2.

10   For the case of 2,3-DHF, the same mechanism is observed in the reactions of sCI2 sCI3 with SO_2. First the intermediate adducts, M2 and M3, are generated and then they evolve through two possible reaction pathways: through the transition state TS2.1 (or TS3.1) or transition state TS2.2 (or TS3.2) resulting in production of SO_3 and an aldehyde or SO_2 and an organic acid respectively. In both cases, similarly to what has been described previously for sCI1, the regeneration of the SO_2 and an organic acid is the more favorable pathway since the intermediate states lie below the energy of reactants. The reaction energies

15   are -116.39 and -115.45 kcal mol^{-1} for the organic acids 2 and 3, respectively, Table 2.

These theoretical results are consistent with the experimental findings described previously: evidences of SO_3 release were not observed and SO_2 concentrations remained unchanged during the laboratory experiments. Thus, both computational and experimental results suggest that SOA formation may generate from reaction (R4) for both 2,5-DHF and 2,3-DHF ozonolysis reactions. Concerning the organic acids from reaction (4),"organic acids 1", "2" and "3": $HC(O)CH_2OCH_2C(O)OH$

20   (formylmethoxyacetic acid), $HC(O)OCH_2CH_2COOH$ (3-formyloxypropanoic acid) and $HC(O)CH_2CH_2OCOOH$ (2-formyl-etoxyformic acid), Fig. 5, there are no vapor pressure data available in the literature. Similar chemicals like $HC(O)OCH(CH_3)COOH$ (2-formyloxy-propionic acid and $CH_3C(O)OCH_2COOH$ (acetoxyacetic acid) are solids at room temperature and have high melting and boiling points (Zanesco, 1966; Buckingham and Donaghy, 1982). Furthermore, previous works (Donahue et al., 2011) provide correlations to estimate vapour pressures based on group contributions factors

25   and oxygenation ratio O:C. For the involved acids, with four carbon atoms and 4 oxygen atoms (1:1 O:C ratio), saturation concentrations as low as 5×10^{11} molecule cm^{-3} are predicted. Thus, the organic acids expected from the SO_2 catalytic pathway could be the species responsible for the nucleation events observed under laboratory conditions.

4. Conclusions.

2,5-DHF and 2,3-DHF show a different behaviour during the ozonolysis showing that the reactivity of the CI is clearly

30   dependent on the structure. For 2,5-DHF the mass increase of particulate matter correlates in time with the total

concentration of reacted alkene. On the other hand, for 2,3-DHF, the particle mass concentration rises well after the total consumption of this cyclic alkene. Furthermore, no effect of RH on the production of SOA was found for the ozonolysis of 2,5-DHF while the increase of RH inhibits the SOA production from to the ozonolysis of 2,3-DHF.

As found in this work, the experimental results for the reaction of ozone with 2,5-DHF show that the presence of small amounts of SO_2 is required to generate SOA. Nevertheless, the main atmospheric fate of 2,5-DHF is the reaction with OH radicals and, so, a small contribution to new particle formation in the atmosphere is expected from reaction (R1). Nevertheless, the information reported in this work contributes to the sparse current knowledge of the reactivity of CI intermediates with SO_2 and H_2O and so it may be helpful in the understanding of the behaviour of other cyclic alkenes.

On the other hand, reaction (R2) is dominant over the OH reaction in the troposphere and, as it has been found in this work, the ozonolysis of 2,3-DHF leads to the formation of SOA in the presence of SO_2. The results show that under increasing amounts of water vapour the yields of SOA decrease, suggesting the competing reactions of the sCI with SO_2 and water molecules.

The experimental findings reported in this work show that SO_2 participates as a catalyst in the in the production of new particles from the ozonolysis of both 2,5-DHF and 2,3-DHF. Under the experimental conditions in this study, at least for the experiments with low SO_2 concentrations, the oxidation of SO_2 to SO_3 through reaction with the corresponding sCI seems negligible, contrary to the results found for smaller carbonyl oxides (Berndt et al., 2014b). Likewise, the pathway producing ester sulfinic acids (reaction (5)) can be ruled out for 2,5-DHF and 2,3-DHF. Thus, the organic acids produced through reaction (4) are expected to be the key species in the formation of SOA.

Acknowledgments.

This work was supported by the Spanish Ministerio de Ciencia e Innovación (project CGL2014-57087-R) and by the University of Castilla La Mancha (projects GI20152950 and GI20163433).

References:

Alwe, H. D., Walavalkar, M. P., Sharma, Dhanya, A. S., Naik P. D.: Tropospheric oxidation of cyclic unsaturated ethers in the day-time: Comparison of the reactions with Cl, OH and O3 based on the determination of their rate coefficients at 298 K, Atmos. Environ., 82, 113-120, 2014.

Anglada, J. M., González, J.,Torrent-Sucarrat, M.: Effects of the substituents on the reactivity of carbonyl oxides. A theoretical study on the reaction of substituted carbonyl oxides with water, Phys. Chem. Chem. Phys., 13, 13034–13045, 2011.

Aranda, A, Díaz-de-Mera, Y., Notario, A., Rodríguez D., Rodríguez, A.: Fine and ultrafine particles in small cities. A case study in the south of Europe, Environ. Sci. Poll. Res., 22 (23), 18477-18486, 2015.

11.

Bartlett, R. J.: Coupled-cluster approach to molecular structure and spectra: a step toward predictive quantum chemistry, J. Phys. Chem., 93 (5), 1697-1708, 1989.

Berndt, T, Jokinen, T., Sipilä, M., Mauldin, R. L., Herrmann, H., Stratmann, F., Junninen, H., Kulmala, M.: H_2SO_4 formation from the gas-phase reaction of stabilized Criegee Intermediates with SO_2: Influence of water vapour content and temperature, Atmos. Environ.. 89, 603-612, 2014a.

Berndt, T., Voigtländer, J., Stratmann, F., Junninen, H., Mauldin, R. L., Sipilä, M., Kulmala, M., Herrmann, H.: Competing atmospheric reactions of CH_2OO with SO_2 and water vapour, Phys. Chem. Chem. Phys., 16, 19130-19136, 2014b.

Boese, A. D., Martin, J. M. L.: Development of Density Functionals for Thermochemical Kinetics. J. Chem. Phys., 121, 3405−3416. 2004.

Boy , M., Mogensen, D., Smolander, S., Zhou, L., Nieminen, T., Paasonen, P., Plass-Dülmer, C., Sipilä, M. J., Petaja, T., Mauldin, R., Berresheim, H., Kulmala, M.: Oxidation of SO_2 by stabilized Criegee intermediate (sCI) radicals as a crucial source for atmospheric sulfuric acid concentrations, Atmos. Chem. Phys., 13(7), 3865-3879, 2013.

Buckingham, J., Donaghy, S.M. Dictionary of Organic Compounds: Fifth Edition, Chapman and Hall, New York, 1982.

Cizek J.: On the Use of the Cluster Expansion and the Technique of Diagrams in Calculations of Correlation Effects in Atoms and Molecules, Adv. Chem. Phys., 14, 35, 1969.

Chan, A. W. H., Chan, M. N., Surratt, J. D., Chhabra, P. S., Loza, C. L., Crounse, J. D., Yee, L. D., Flagan, R. C., Wennberg, P. O., Seinfeld, J. H.: Role of aldehyde chemistry and NOx concentrations in secondary organic aerosol formation, Atmos. Chem. Phys., 10, 7169–7188, 2010.

Chao, W., Hsieh, J. T., Chang, C. H., Lin, J. M.: Direct kinetic measurement of the reaction of the simplest Criegee intermediate with water vapor, Science, 347 (6223), 751-754, 2015.

Donahue, N. M., Epstein, S. A., Pandis, S. N., and Robinson, A. L.: A two-dimensional volatility basis set: 1. organic-aerosol mixing thermodynamics, Atmos. Chem. Phys., 11, 3303–3318, 2011.

Ehn, M., Thornton, J. A., Kleist, E., Sipila, M., Junninen, H., Pullinen, I., Springer, M., Rubach, F., Tillmann, R., Lee, B., Lopez-Hilfiker, F., Andres, S., Acir, I. H., Rissanen, M., Jokinen, T., Schobesberger, S., Kangasluoma, J., Kontkanen, J., Nieminen, T., Kurten, T., Nielsen, L. B., Jorgensen, S., Kjaergaard, H. G., Canagaratna, M., Maso, M. D., Berndt, T., Petaja, T., Wahner, A., Kerminen, V. M., Kulmala, M., Worsnop, D. R., Wildt, J., and Mentel, T. F.: A large source of low-volatility secondary organic aerosol, Nature, 506, 476–479, 2014.

Fan, X., Wang, X., Yang, K., Li, L., Wu, C., Li, Z.: Experimental and Modeling Study on Ignition Characteristics of 2, 5-Dihydrofuran, SAE International Journal of Fuels and Lubricants, 9(1), 315-321, 2016.

Freitas, S.R., Longo, K. M., Alonso, M. F., Pirre, M., Marecal, V., Grell, G., Stockler,R., Mello, R. F., Gacita M.S.: PREP-CHEM-SRC – 1.0: A preprocessor of trace gas and aerosol emission fields for regional and global atmospheric chemistry models, Geosci. Model Dev., 4, 419–433, 2011.

Frisch, M. J., Trucks, G. W., Schlegel, H. B., Scuseria, G. E., Robb, M. A., Cheeseman, J. R., Scalmani, G., Barone, V., Mennucci, B., Petersson, G. A. et al.: Gaussian 09, revision A.02, Gaussian, Inc: Wallingford, CT, 2009.

Jiang, L., Xu, Y., Ding, A.: Reaction of stabilized Criegee intermediates from ozonolysis of limonene with sulfur dioxide: ab initio and DFT study, J. Phys. Chem. A, 114, 12452-12461, 2010.

Jayne, J. T., Po1schl, U., Chen, Y., Dai, D., Molina, L.T., Worsnop, D.R., Kolb, C.E., Molina, M. J.: Pressure and Temperature Dependence of the Gas-Phase Reaction of SO3 with H2O and the Heterogeneous Reaction of SO3 with H2O/H2SO4 Surfaces. J. Phys. Chem. A, 101, 10000-10011, 1997.

Johnson, D., Marston, G.: The gas-phase ozonolysis of unsaturated volatile organic compounds in the troposphere, Chem. Soc. Rev., 37, 699–716, 2008.

Kurtén, T., Lane, J. R., Jørgensen, S., Kjaergaard, H. G.: A Computational Study of the Oxidation of SO_2 to SO_3 by Gas-Phase Organic Oxidants, J. Phys. Chem. A, 115 (31), 8669–8681, 2011.

Lemieux, P. M., Lutes, C. C., Santoianni, D. A.: Emissions of organic air toxics from open burning: A comprehensive review, Prog. in Energy Combust. Sci., 30, 1–32, 2004.

Liu, T., Wang, X., Hu, Q., Deng, W., Zhang, Y., Ding, X., Fu, X., Bernard, F., Zhang, Z., Lü, S., He, Q., Bi, X., Chen, J., Sun, Y. Yu, J., Peng, P., Sheng, G., Fu, J.: Formation of secondary aerosols from gasoline vehicle exhaust when mixing with SO_2, Atmos. Chem. Phys., 16, 675–689, 2016.

Loza, C. L., Craven, J. S., Yee, L.D., Coggon, M. M., Schwantes, R. H., Shiraiwa, M., Zhang, X., Schilling, K. A., Ng4, N.L., Canagaratna, M. R., Ziemann, P. J., Flagan, R. C., Seinfeld, J. H.: Secondary organic aerosol yields of 12-carbon alkanes, Atmos. Chem. Phys., 14, 1423–1439, 2014.

Ma, Y., Porter, R. A., Chappell, D., A. T. Andrew, Russell, T., Marston G.: Mechanisms for the formation of organic acids in the gas-phase ozonolysis of 3-carene, Phys. Chem. Chem. Phys., 11, 4184–4197, 2009.

Martín, P., Tuazon, E. C.: Aschmann, S. M. Arey, J., Atkinson, R.: Formation and Atmospheric Reactions of 4,5-Dihydro-2-methylfuran, J. Phys. Chem. A 106, 11492-11501, 2002.

Mauldin, R. L., Berndt, T., Sipilä, M., Paasonen, P., Petäjä, T., Kim, S., Kurtén, T., Stratmann, F., Kerminen, V. M., Kulmala, M.: A new atmospherically relevant oxidant of sulphur dioxide, Nature, 488, 193–196, 2012.

Metzger, A., Verheggen, B., Dommen, J., Duplissy, J., Prevota, A. S. H., Weingartner, E.,Riipinen, I, Kulmala, M., Spracklend, D. V., Carslaw, K. S., Baltensperger, U.: Evidence for the role of organics in aerosol particle formation under atmospheric conditions. PNAS., 107, 6646-6651, 2010.

Newland, M. J., Rickard, A. R., Vereecken, L., Muñoz, A., Ródenas, M., Bloss, W. J.: Atmospheric isoprene ozonolysis: impacts of stabilised Criegee intermediate reactions with SO_2, H_2O and dimethyl sulfide, Atmos. Chem. Phys., 15, 9521-9536, 2015a.

Newland, M. J., Rickard, A. R., Alam, M. S., Vereecken, L. Muñoz, A., Ródenas, M., Bloss, W.J.: Kinetics of stabilised Criegee intermediates derived from alkene ozonolysis: reactions with SO_2, H_2O and decomposition under boundary layer conditions, Phys. Chem. Chem. Phys., 17, 4076-4088, 2015b.

Pruppacher, H. R., Klett, J. D., Wang, P. K.: Microphysics of Clouds and Precipitation, Aerosol Sci. Tech., 28(4), 381-382, 1998.

Román-Leshkov, Y., Barrett, C. J., Liu, Z. Y., Dumesic, J. A.: Production of dimethylfuran for liquid fuels from biomass-derived carbohydrates, Nature, 447(7147), 982-985, 2007.

Ryzhkov, B., Ariya, P. A.: A theoretical study of the reactions of parent and substituted Criegee intermediates with water and the water dimer, Phys. Chem. Chem. Phys., 6, 5042-5050, 2004.

Saathoff, H., Naumann, K. H., Möhler, O., Jonsson, A, M., Hallquist, M., Kiendler-Scharr, A., Mentel, T. F., Tillmann, R., Schurath, U.: Temperature dependence of yields of secondary organic aerosols from the ozonolysis of -pinene and limonene, Atmos. Chem. Phys, 9, 1551–1577, 2009.

Sipilä, M., Jokinen, T., Berndt, T., Richters, S., Makkonen, R., Donahue, N. M., Mauldin, R. L, Kurtén, T., Paasonen, P., Sarnela, N., Ehn, M., Junninen, H., Rissanen, M. P., Thornton, J., Stratmann, F., Herrmann, H., Worsnop, D. R., Kulmala, M., Kerminen, V. M., Petäjä, T.: Reactivity of stabilized Criegee intermediates (sCIs) from isoprene and monoterpene ozonolysis toward SO_2 and organic acids, Atmos. Chem. Phys., 14, 12143–12153, 2014.

Stone, D., Blitz, M., Daubney, L., Howes, N, U., Seakins, P.: Kinetics of CH_2OO reactions with SO_2, NO_2, NO, H_2O and CH_3CHO as a function of pressure, Phys. Chem. Chem. Phys., 16, 1139-1149, 2014.

Vereecken, L., Harder, H., Novelli, A.: The reaction of Criegee intermediates with NO, RO_2, and SO_2, and their fate in the atmosphere, Phys. Chem. Chem. Phys., 14, 14682–14695, 2012.

Welz, O., Savee, J. D., Osborn, D. L., Vasu, S. S., Percival, C. J, Shallcross, D., Taatjes, C.: Reaction of CH_2I with O_2 forms Criegee Intermediate: Direct Measurements of CH_2OO Kinetics, Science, 335, 204-207, 2012.

Zanesco, C. R.: Oxydation des aldéhydes α, β-non-saturés par l'acide peroxoacétique, Helv. Chim. Acta, 49, 1002-1012, 1966.

Zhang, X., Schwantes, R. H., Coggon, M. M., Loza, C. L., Schilling, K. A., Flagan, R. C., Seinfeld, J. H.: Role of ozone in SOA formation from alkane photooxidation, Atmos. Chem. Phys., 14, 1733–1753, 2014.

Table 1. Initial concentrations of reactants and SOA data for the ozonolysis reaction of 2,3-DHF. PNC, PMC and diameter reported values are the maximum data registered for each magnitude during the experiment. All the experiments reported in this table were carried out under HR=0.

2,3-DHF (ppm)	O_3 (ppm)	SO_2 (ppm)	PNC (#/cm³)	PMC (µg/m³)	Diameter (nm)
0.2	0.5	0.5	5.7×10^6	2	25
0.5	0.5	0.5	5.8×10^5	1.9	30
1	0.5	0.5	3.0×10^4	0	-
2	0.5	0.5	1.0×10^3	0	-
3	0.2	0.5	27	0	-
3	0.5	0.5	47	0	-
3	1	0.5	5.3×10^3	0.12	80
0.5	1	0.5	1.70×10^6	10.1	40
0.5	2	0.5	2.10×10^6	18.9	50
0.5	3	0.5	3.30×10^6	33.5	50
0.5	4	0.5	3.40×10^6	38	60

Table 2. Relative energies to reactants sCI and SO_2 ($\Delta E + ZPE$) in kcal mol^{-1} for stationary points of the all reaction. Energies were obtained at CCSD(T)/6-311G(d,p) level of theory and zero point energies were obtained at BMK/6-311++G(3df,3pd) level of theory.

	A	B	C	D	D'	E	E'
sCI1	72.21	2.57	-30.39	-12.58	-8.42	-59.58	-117.58
sCI2	93.45	2.01	-28.01	-11.32	-9.40	-55.87	-116.39
sCI3	93.45	2.01	-26.61	-10.32	-6.07	-69.28	-115.45
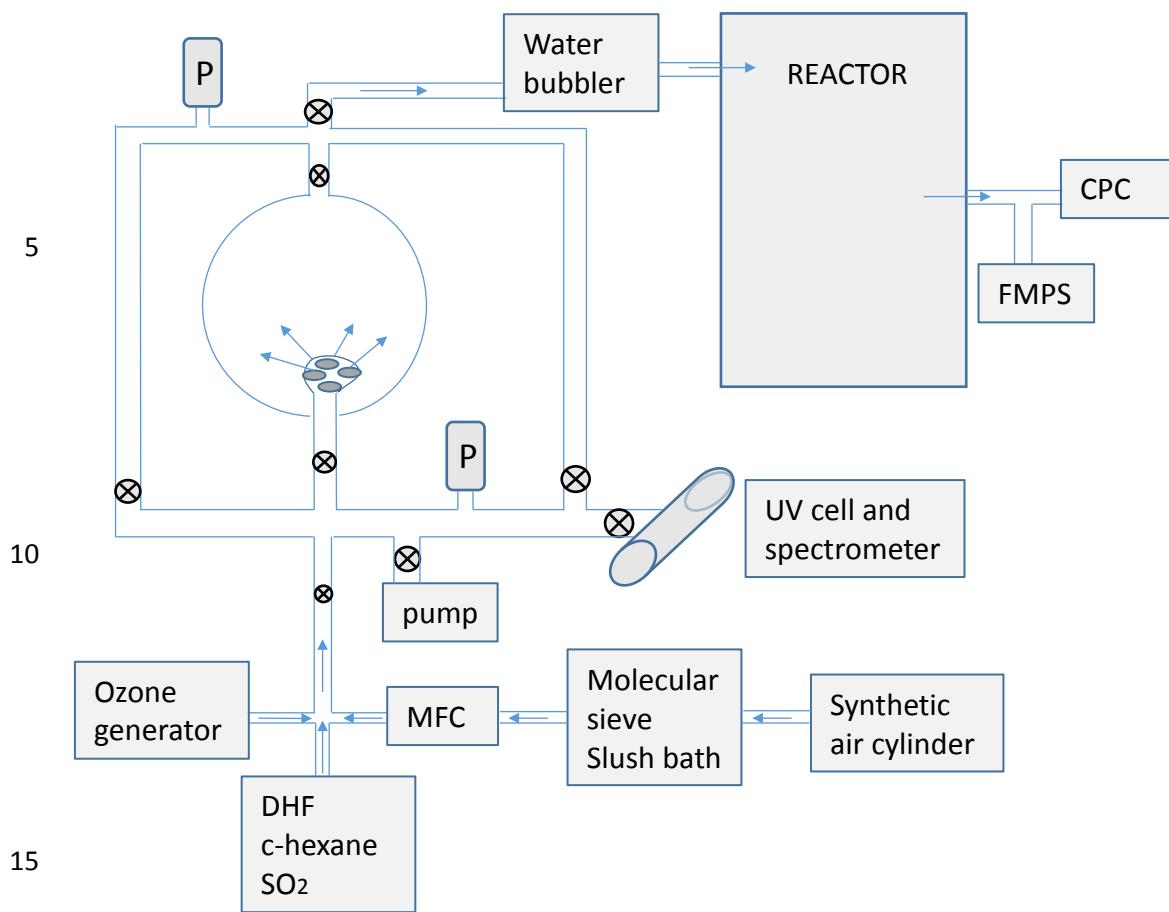
Figure 1. Schematic set-up of the experimental system.
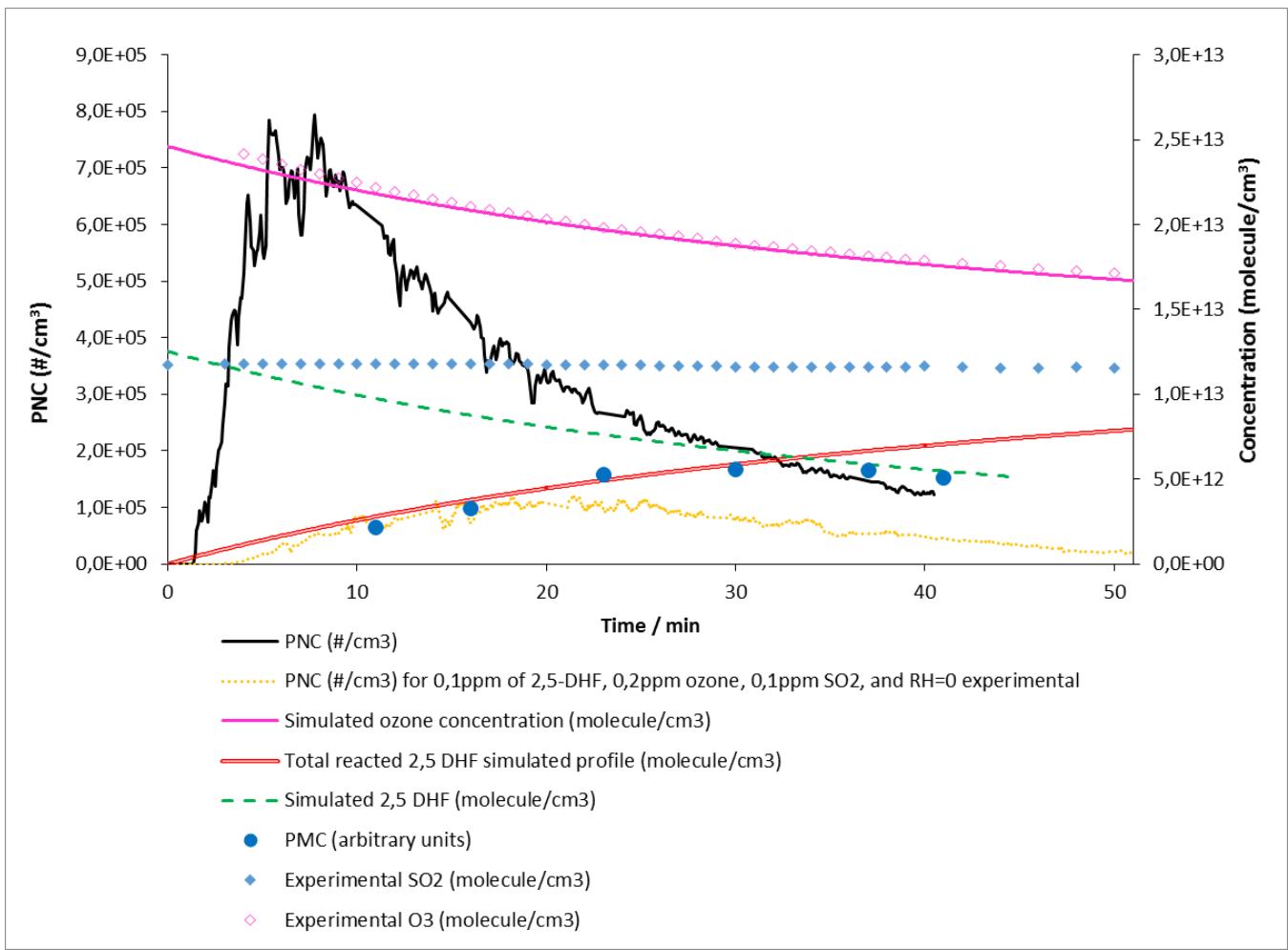
Figure 2. Temporal profiles for particles and gases. Initial concentrations: 0.5ppm of 2,5-DHF, 1ppm of O_3, 0.5ppm of SO_2 and RH= 0.
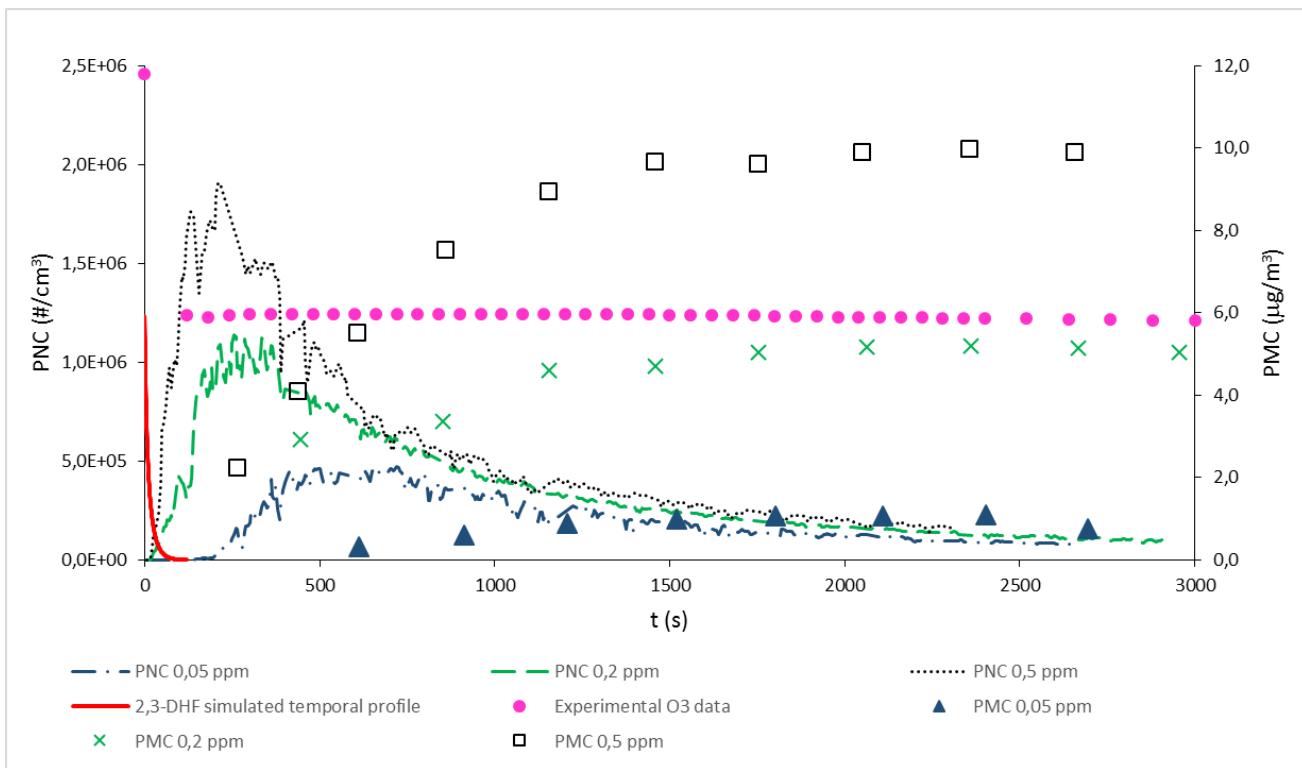
Figure 3. PNC and PMC profiles for different SO_2 initial concentrations (0.05, 0.2 and 0.5 ppm). This series of experiments was carried out under dry conditions and with 0.5 ppm of 2,3-DHF and 1 ppm of ozone initial concentrations. Simulated temporal profile of 2,3-DHF, red solid line.
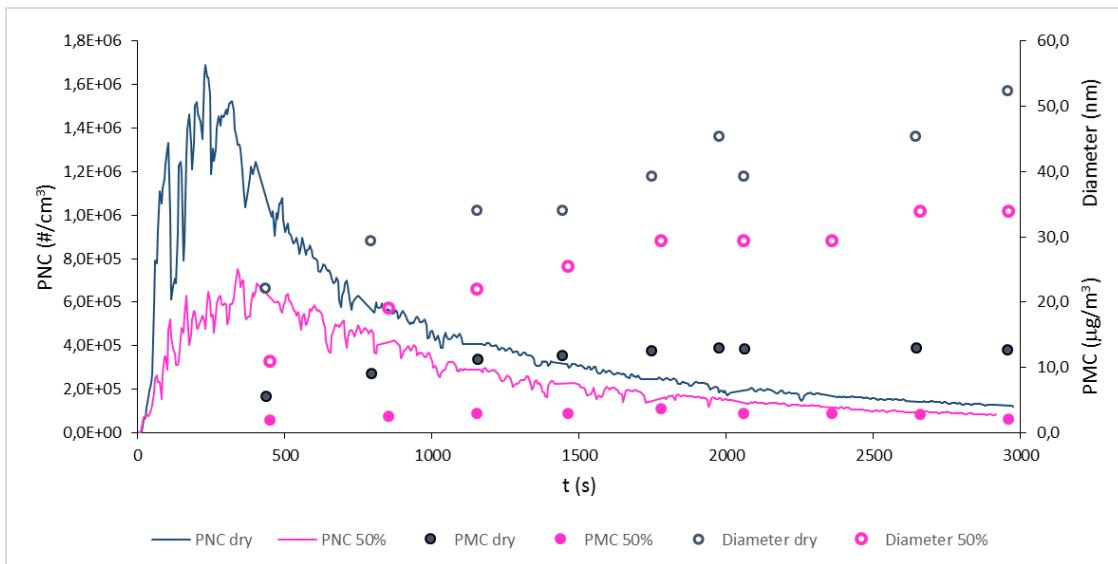
Figure 4. Effect of water vapour on PNC, PMC and on the particle diameters' profiles: dry conditions versus 50% HR. Both experiments were carried out with 0.5, 1.0 and 0.5 ppm initial concentrations of 2,3-DHF, ozone and SO_2 respectively.
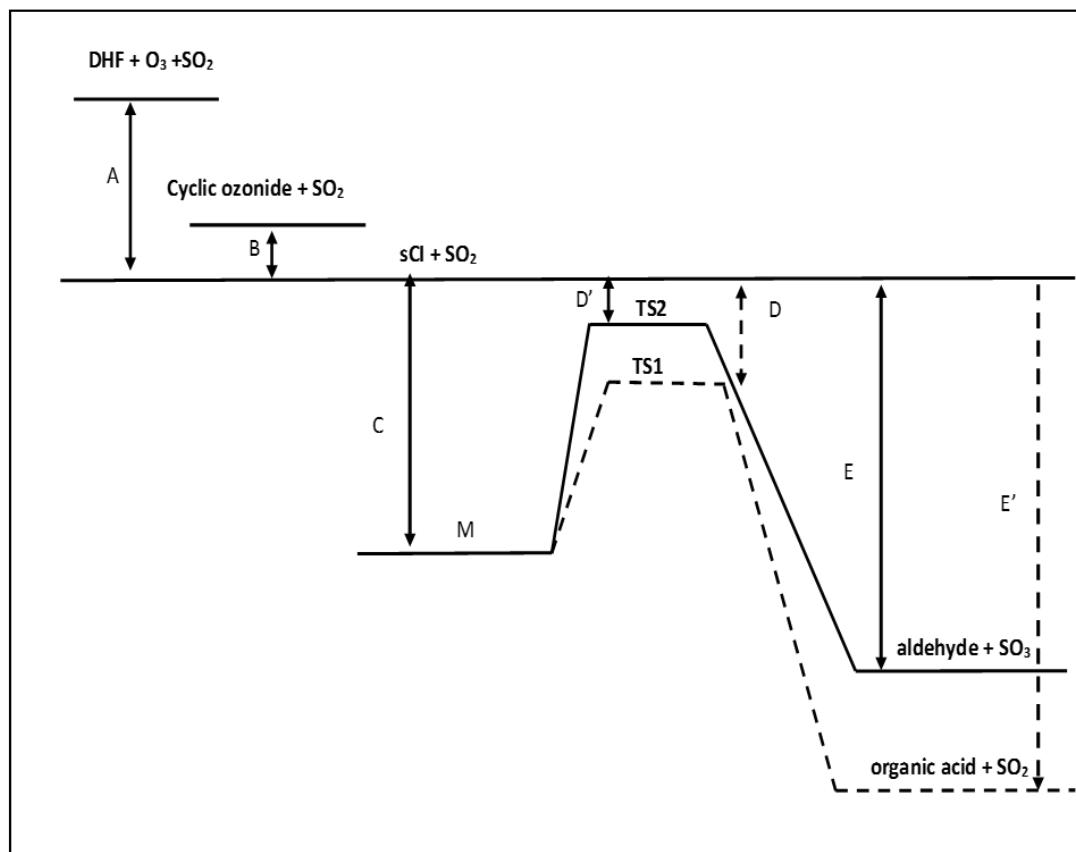
Figure 5a. General schematic potential energy surface for the reactions sCI + SO$_2$ → Products.

i) 2,5-DHF

sCI1   M1   TS1.1   TS1.2   Organic acid 1   Aldehyde 1

ii) 2,3-DHF

sCI2   M2   TS2.1   TS2.2   Organic acid 2   Aldehyde 2

sCI3   M3   TS3.1   TS3.2   Organic acid 3   Aldehyde 3
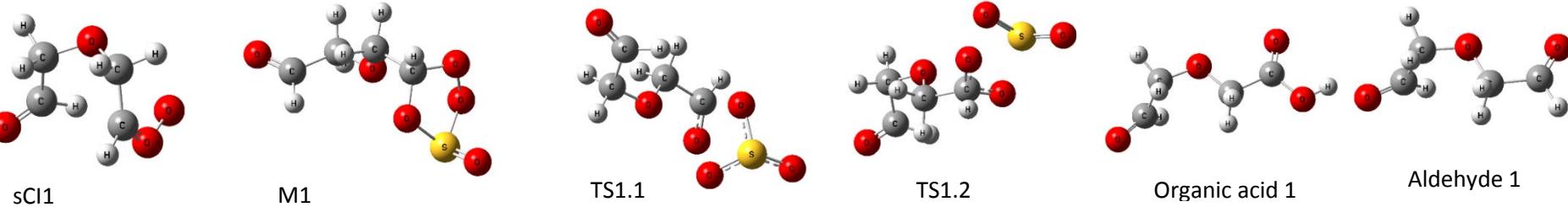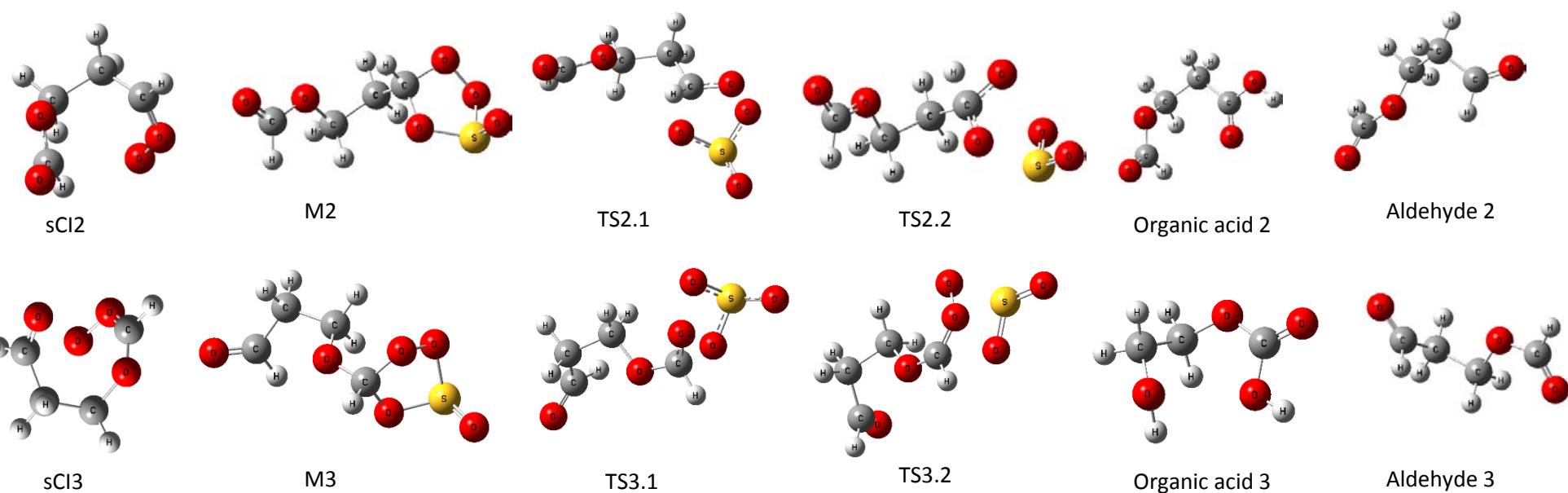
Figure 5b. Geometries of stationary points involved in the sCI + SO_2 reaction at BMK/6-311++G(3df,3pd) level of theory.